Numerical results on the density fluctuations in liquid rubidium

L. Sjögren
Institute of Theoretical Physics, Chalmers University of Technology, S-412 96 Göteborg, Sweden
(Received 31 March 1980)

Numerical results for the dynamic structure factor $S(q\omega)$ in liquid rubidium are presented based on a kinetic theory presented in an earlier paper. The results are in quantitative agreement with those obtained from molecular dynamics calculations and experiments. In the theory, different dynamical processes such as single binary collisions and nonlinear couplings to density and current fluctuations, are separated, and we investigate their relative contributions to the relevant memory function, as well as their effect on the shape of $S(q\omega)$.

I. INTRODUCTION

In three recent papers,[1-3] we presented a microscopic kinetic theory to describe the self-motion and the current fluctuations in monatomic classical liquids. In the present paper we present numerical results for the dynamical structure factor $S(q\omega)$ in liquid rubidium based on this theory, and we compare our results with those obtained from MD (molecular dynamics) calculations[4] and neutron scattering experiments.[5]

Liquid rubidium has been extensively studied during the past years through various approaches[6-12] and its behavior is therefore relatively well understood. The main purpose with the present paper is, therefore, to test the accuracy of the approximations introduced in papers I and III and to compare with our earlier results on this system.[12] Also, since the relevant memory function in our theory is separated in a binary-collision part and a part describing repeated correlated collisions, we are able to investigate how the different dynamical processes, i.e., binary collisions, nonlinear coupling to density fluctuations, etc., will influence the detailed shape of $S(q\omega)$.

The present calculations have been performed for small and intermediate wave vectors, where $S(q\omega)$ show a pronounced structure due to collective effects. For larger-q values the dynamics is to a large extent determined by the self-motion, and is therefore less sensitive to the details of our approximations. This fact is demonstrated by our earlier results for $S(q\omega)$,[12] which gave very good agreement with experiments for $q > 1.25$ Å^{-1}, but gave rather large discrepancies for smaller-q values.

II. BASIC FORMULAS

In this section we collect all the relevant formulas needed in our calculations and for their derivation we refer to papers I and III. For the dynamical structure factor we have

$$S(q\omega) = (1/\pi)\,\mathrm{Re}F(q, z = -i\omega)\,, \tag{2.1}$$

where $F(qz)$, the Laplace transform of the intermediate scattering function, is given by [see III: (2.24) and (2.26)]

$$F(qz) = S(q)\frac{F^s(qz) - (\beta m/q^2)\Gamma^d_{11}(qz)[zF^s(qz) - 1]}{1 + [nc(q) - (\beta m z/q^2)\Gamma^d_{11}(qz)][zF^s(qz) - 1]}\,. \tag{2.2}$$

Here F^s denotes the self-part of F, and $S(q)$ and $c(q)$ are the static structure factor and the direct correlation function, respectively, n is the average density, $\beta = (k_BT)^{-1}$ is the inverse temperature, and m denotes the atomic mass. The memory function Γ^d_{11}, which generalizes the ordinary mean-field result,[13] describes the backflow around any single atom[14] and is given by

$$\Gamma^d_{11}(qz) = \Gamma_{11}(qz) - \Gamma^s_{11}(qz)\,, \tag{2.3}$$

where Γ_{11} and Γ^s_{11} are matrix elements, representing the longitudinal current of the memory functions for the respective phase-space correlation functions. In papers I and III we derived explicit expressions for these matrix elements in terms of a binary-collision part and various mode-mode coupling integrals. For Γ^s_{11} we have [see I: (4.8)]

$$\Gamma^s_{11}(qz) = \frac{\Gamma^{sB}_{11}(qz) + R^s_{00}(qz) + \Gamma^{sB}_{11}(qz)R^s_{01}(qz)}{1 - R^s_{01}(qz) - \Gamma^{sB}_{11}(qz)[R^s_{11}(qz) + R^s_{22}(qz)]}\,. \tag{2.4}$$

Actually the derivation in I was performed for $q = 0$ but it also works as well for $q \neq 0$. Moreover, in (2.4) we have neglected the renormalizations of the coefficient before R^s_{22} from the longitudinal modes, since in paper II this was found to give a negligible numerical effect for short and intermediate times at the present density. In (2.4) Γ^{sB}_{11} represents one binary-collision process with a rapid time dependence and it is, as in

paper II, approximated with a simple Gaussian ansatz

$$\Gamma_{11}^{sB}(qt) = \omega_0^2 \exp[-t^2/\tau_s^2(q)] . \tag{2.5}$$

Here ω_0^2 is the Einstein frequency

$$\omega_0^2 = \frac{n}{3m} \int d\vec{r}\, g(r) \nabla^2 v(r) , \tag{2.6}$$

with $v(r)$ and $g(r)$ denoting the interatomic potential and the static pair distribution function, respectively. The relaxation time $\tau_s(q)$, obtained from a short-time expansion, is given by [see I: (A1.11)]

$$\omega_0^2 \tau_s^{-2}(q) = \left(\frac{q^2}{2\beta m}\right)\omega_0^2 + \left(\frac{n}{3m^2}\right) \times \int d\vec{r}\,[\nabla^\alpha \nabla^\beta v(r)] g(r) [\nabla^\alpha \nabla^\beta v(r)] + \frac{1}{6n} \int \frac{d\vec{q}'}{(2\pi)^3} \gamma_d^{\alpha\beta}(q') [S(q') - 1] \gamma_d^{\alpha\beta}(q') , \tag{2.7}$$

where summation over repeated indices is implied. Here $\gamma_d^{\alpha\beta}(q)$ is given by

$$\gamma_d^{\alpha\beta}(q') = -\left(\frac{n}{m}\right) \int d\vec{r} \exp(-i\vec{q}' \cdot \vec{r}) g(r) \nabla^\alpha \nabla^\beta v(r) = \hat{q}'^\alpha \hat{q}'^\beta \gamma_d^l(q') + (\delta_{\alpha\beta} - \hat{q}'^\alpha \hat{q}'^\beta) \gamma_d^t(q') . \tag{2.8}$$

The mode-mode integrals denoted by R^s in (2.4) contains the nonlinear coupling to the density and current fluctuations. R_{00}^s couples to the density fluctuations and is given by

$$R_{00}^s(qt) = \frac{n}{\beta m} \int \frac{d\vec{q}}{(2\pi)^3} (\hat{q} \cdot \vec{q}')^2 [c(\vec{q}')]^2 \times [F^s(\vec{q} - \vec{q}', t) F(\vec{q}' t) - F^0(\vec{q} - \vec{q}', t) F^B(\vec{q}' t)] , \tag{2.9}$$

where F^0 is the free-particle expression of F and

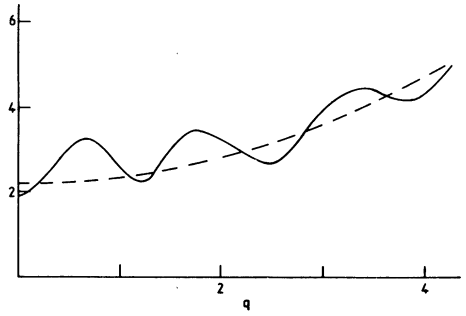

FIG. 1. Relaxation times $\tau_l^{-2}(q)$ (full curve) and $\tau_s^{-2}(q)$ (dashed curve) versus q. The vertical axis is in units of τ_0^{-2} where $\tau_0 = 3.212 \times 10^{-13}$ sec is the time unit used also in all subsequent figures. The wave vector is in units of Å^{-1}.

F^B is given by

$$F^B(qt) = [F^0(qt)/F^s(qt)] F(qt) . \tag{2.10}$$

In papers I and II we used the approximation $F^B = F$ instead of (2.10). However, as was discussed in III, that approximation cannot be used when calculating $S(q\omega)$, since the mode-mode integrals in Γ_{11} would vanish [see Eqs. (2.15)–(2.20) below].

For R_{01}^s we have

$$R_{01}^s(qt) = -\int \frac{d\vec{q}'}{(2\pi)^3} (\hat{q} \cdot \hat{q}')^2 c(\vec{q}') \times \left[\gamma_d^l(\vec{q}') + \left(\frac{q'^2}{\beta m}\right) nc(\vec{q}')\right] \omega_0^{-2} \times [F^s(\vec{q} - \vec{q}', t) - F^0(\vec{q} - \vec{q}', t)] \frac{\partial}{\partial t} F(\vec{q}' t) . \tag{2.11}$$

R_{11}^s and R_{22}^s contain the coupling to the longitudinal and transverse current-correlation functions, respectively, and are given by

$$R_{11}^s(qt) = -\frac{1}{n} \int \frac{d\vec{q}'}{(2\pi)^3} (\hat{q} \cdot \hat{q}')^2 \left[\gamma_d^l(\vec{q}') + \left(\frac{q'^2}{\beta m}\right) nc(\vec{q}')\right]^2 \omega_0^{-4} \times [F^s(\vec{q} - \vec{q}', t) - F^0(\vec{q} - \vec{q}', t)] C_l(\vec{q}' t) \tag{2.12}$$

and

$$R_{22}^s(qt) = -\frac{1}{n} \int \frac{d\vec{q}'}{(2\pi)^3} [1 - (\hat{q} \cdot \hat{q}')^2] [\gamma_d^t(\vec{q}')]^2 \omega_0^{-4} \times [F^s(\vec{q} - \vec{q}', t) - F^0(\vec{q} - \vec{q}', t)] C_t(\vec{q}' t) , \tag{2.13}$$

where C_l and C_t denote the longitudinal and transverse current-correlation functions, respectively, normalized to unity for $t = 0$.

For Γ_{11} we have an expression similar to (2.4) [see III: (3.33)]:

$$\Gamma_{11}(qz) = \frac{\Gamma_{11}^B(qz) + R_{00}^l(qz) + \Gamma_{11}^B(qz) R_{01}^l(qz)}{1 - R_{01}^l(qz) - \Gamma_{11}^B(qz)[R_{11}^l(qz) + R_{22}^l(qz)]} . \tag{2.14}$$

For the binary part Γ_{11}^B we again make a simple Gaussian ansatz:

$$\Gamma_{11}^B(qt) = [\omega_0^2 + \gamma_d^l(q) + (q^2/\beta m) nc(q)] \times \exp[-t^2/\tau_l^2(q)] . \tag{2.15}$$

The relaxation time $\tau_l(q)$ can again be determined from a short-time expansion similar to $\tau_s(q)$ in (2.7) and the result, which is related to the sixth moment of $S(q\omega)$, was given in III [Eq. (3.22)]. It turns out that τ_l and τ_s have approximately the same overall magnitude, except that $\tau_l(q)$ has an oscillatory q dependence as is shown in Fig. 1.

These oscillations reflect the initial static structure, which is even more pronounced in $\Gamma^B_{11}(q, t=0)$. Actually, both $\tau_l(q)$ and $\tau_s(q)$ should represent a binary-collision time, and we do not expect this to be very sensitive to the q value considered. For this reason, we will take here $\tau_l(q) = \tau_s(q)$, which also lead to somewhat better numerical results for $S(q\omega)$.

For the mode-mode integrals in (2.14) we have [see III: (3.34)–(3.37)]

$$R^l_{00}(qt) = \frac{n}{\beta m}\int \frac{d\vec{q}'}{(2\pi)^3}\,\hat{q}\cdot\vec{q}'c(\vec{q}') \times[\hat{q}\cdot\vec{q}'c(\vec{q}')+\hat{q}\cdot(\vec{q}-\vec{q}')c(\vec{q}-\vec{q}')] \times[F(\vec{q}-\vec{q}',t)F(\vec{q}'t) - F^B(\vec{q}-\vec{q}',t)F^B(\vec{q}'t)], \tag{2.16}$$

which is similar to (2.9), except that we have an additional exchange term in the coupling constant and also that F^s and F^0 have been replaced with F and F^B, respectively. For R^l_{01} we have

$$R^l_{01}(qt) = \int \frac{d\vec{q}'}{(2\pi)^3}\,\frac{\hat{q}^\beta\hat{q}'^\alpha}{q'}\,t^{\alpha\beta}(\vec{q}\vec{q}') \times[\hat{q}\cdot\vec{q}'c(\vec{q}')+\hat{q}\cdot(\vec{q}-\vec{q}')c(\vec{q}-\vec{q}')] \times[F(\vec{q}-\vec{q}',t)-F^B(\vec{q}-\vec{q}',t)]\frac{\partial}{\partial t}F(\vec{q}'t), \tag{2.17}$$

where the coupling constant $t^{\alpha\beta}$ is given by

$$t^{\alpha\beta}(\vec{q}\vec{q}') = \frac{\gamma_d^{\alpha\beta}(\vec{q}-\vec{q}')+(q-q')^\alpha(q-q')^\beta(n/\beta m)c(\vec{q}-\vec{q}')-\gamma_d^{\alpha\beta}(\vec{q}')-q'^\alpha q'^\beta(n/\beta m)c(\vec{q}')}{\omega_0^2+\gamma_d^l(\vec{q})+q^2(n/\beta m)c(\vec{q})} \tag{2.18}$$

The couplings to the currents are given by

$$R_{11}(qt) = -\frac{1}{n}\int \frac{d\vec{q}'}{(2\pi)^3}\,\hat{q}^\gamma\hat{q}^\delta\hat{q}'^\alpha\hat{q}'^\beta t^{\alpha\gamma}(\vec{q}\vec{q}')t^{\beta\delta}(\vec{q}\vec{q}') \times[F(\vec{q}-\vec{q}',t)-F^B(\vec{q}-\vec{q}',t)]C_l(\vec{q}'t) \tag{2.19}$$

and

$$R^l_{22}(qt) = -\frac{1}{n}\int \frac{d\vec{q}'}{(2\pi)^3}\,\hat{q}^\gamma\hat{q}^\delta(\delta_{\alpha\beta}-\hat{q}'^\alpha\hat{q}'^\beta)t^{\alpha\gamma}(\vec{q}\vec{q}')t^{\beta\delta}(\vec{q}\vec{q}') \times[F(\vec{q}-\vec{q}',t)-F^B(\vec{q}-\vec{q}',t)]C_t(\vec{q}'t). \tag{2.20}$$

To obtain results from (2.2) we also need an expression for the self-part F^s. We will here use the Gaussian approximation

$$F^s(qt) = \exp\left[-\left(\frac{q^2}{m\beta}\right)\int_0^t dt'(t-t')\Phi(t')\right], \tag{2.21}$$

where $\Phi(t)$ is the normalized velocity correlation function given in terms of its corresponding memory function by

$$[z+\Gamma(z)]\Phi(z) = 1. \tag{2.22}$$

For $\Gamma(z)$ we then have [see I: (2.24)]

$$\Gamma(z) = \Gamma^s_{11}(q=0,z). \tag{2.23}$$

This constitutes our basic formulation for the calculation of $S(q\omega)$. The calculations have been performed at a mass density of 1.503 g cm^{-3} and a temperature of 319 K, which are the same conditions for which Rahman carried out computer simulations,[4] using the effective pair potential obtained by Price *et al.*,[15] and also for which Copley and Rowe[5] performed their experiments. The static quantities that enter into the theory were calculated with the values of $v(r)$, $g(r)$, and $S(q)$ supported by Rahman (private communication). For the dynamical correlation functions entering in the mode-mode integrals we have used the same values as in the earlier calculations of $\Phi(t)$ and $\Gamma(t)$, and we refer to paper II for more details about this.

III. NUMERICAL RESULTS

For reference we show in Fig. 2 the results for $\Gamma(t)$ obtained from Eqs. (2.4)–(2.13) and (2.23) (full curve) together with the MD results of Rahman[4] (dots). This figure should be compared with the corresponding results in paper II. The only difference is that the expression for R^s_{00} is slightly modified by the appearance of F^B, given by Eq. (2.10), instead of F in Eq. (2.9). The overall effect on the time dependence of $\Gamma(t)$ by this change is small, and it just increases the height of the tail around $t = 2.5$ somewhat.

In Fig. 3 we show our present results for $S(q\omega)$ for small and intermediate wave vectors (full curves) together with the MD (Ref. 4) and experimental[5] ($q = 1.25$) results (dots). Comparing with our earlier results in paper IV we see a large improvement, in particular for smaller-q values where the earlier results was not even qualitatively correct. The too-sharp peaks at the two

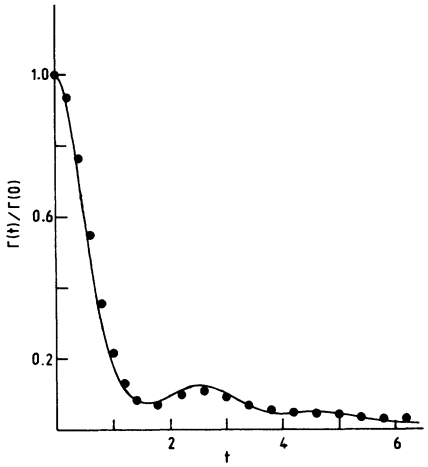

FIG. 2. Normalized memory function for the velocity correlation function versus time. Present results (full curve) and MD results of Rahman (dots). The time is expressed in units of τ_0.

lowest q values in Fig. 3 is mainly due to our neglect of the coupling to temperature fluctuations, which have a large effect at these q values.[11] For the other three q values the present results are more or less quantitatively correct. Some of the remaining discrepancies are due to our inability to reproduce the correct width of the binary part of the memory functions as seen in Fig. 2. If we correct for this defect by changing $\tau_s(q)$, the magnitude of the peaks in Fig. 3 is decreased somewhat and the peak-position is slightly shifted towards larger frequencies. The high-frequency shoulder found at $q=0.797$ and 0.998 may be due to too strong oscillations in our input $F(qt)$. A similar structure was found also

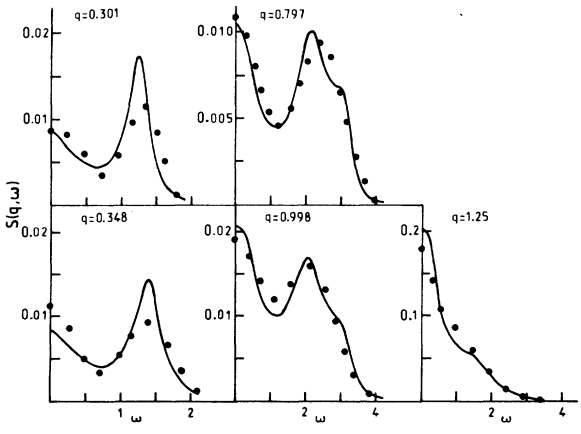

FIG. 3. $S(q\omega)$ versus ω. The present theory is given by the full curves and the MD results of Rahman is given by dots. At $q=1.25$ Å^{-1} the dots denote the experimental results of Copley and Rowe. $S(q\omega)$ is expressed in units of τ_0 and ω in units of τ_0^{-1}.

in our results for $\Phi(\omega)$. To some extent this structure is also found at $q=1.25$ and our results show a more pronounced tendency of a side peak than the experimental data of Copley and Rowe.

In Fig. 4 we show how $S(q\omega)$ varies when different dynamical couplings are introduced into the memory functions. The dots are again the MD and experimental results. The dashed curves show the results for $S(q\omega)$ when only the binary parts in the memory functions Γ_{11}^d and Γ are kept, i.e., all mode-mode integrals R_{00}^s, R_{00}^l, etc., are set equal to zero. We see that the main features of $S(q\omega)$ are reproduced with this approximation, except that the central peak disappears more or less completely for the lower-q values. Including also the coupling to the density fluctuations via R_{00}^s and R_{00}^l into Eqs. (2.4) and (2.14), we obtain the dotted curves in Fig. 4 and the results for $S(q\omega)$ are now in very good agreement with the MD and experimental values even for small frequencies. Including also the longitudinal currents via the mode integrals R_{01} and R_{11} we obtain more or less the final results shown in Fig. 3, i.e., the coupling to the transverse current via R_{22} is very small and has no essential effect on $S(q\omega)$. The effect of the longitudinal currents is to sharpen the side peak and they also make the high-frequency shoulder at $q=0.797$ and 0.998 more pronounced. However, as stated above, this latter effect is probably due to too much oscillations in our input data for $F(qt)$.

It should be noticed that for obtaining the results shown in Fig. 4, the self-part F^s has been calculated with a $\Gamma(z)$ consistent with $\Gamma_{11}^d(qz)$, i.e., the same contributions have been included in both these functions, and this is necessary to preserve momentum conservation. If we were to neglect Γ and Γ_{11}^d completely when calculating $S(q\omega)$ we would obtain the mean-field result of Nelkin and Ranganathan.[16] This result gives side peaks in $S(q\omega)$ due to the mean-field term, but the resonances are too sharp since only Landau damping is included. As expected, the main damping mecha-

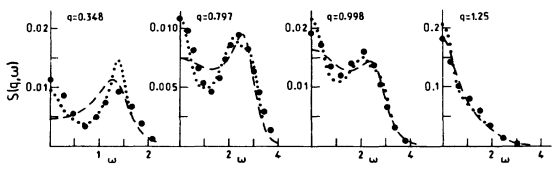

FIG. 4. $S(q\omega)$ versus ω. The dots are the same as in Fig. 3. The dashed curve show the results for $S(q\omega)$ when only single binary collisions are included in the memory functions Γ_{11}^d and Γ. The dotted curves show $S(q\omega)$ when the mode-mode coupling terms R_{00}^s and R_{00}^l are also included in the memory functions.

nism of the resonance is reproduced by including only binary collisions, as is seen from Fig. 4. For smaller-q values the time tail in the memory functions has also a rather large effect on the side peak, which can be understood since collective effects are more important at small-q values.

We will now consider the time dependence of the memory function Γ^d_{11} more closely. The two parts Γ_{11} and Γ^s_{11} in (2.3) have a rather similar time dependence for all q values, and both look more or less like $\Gamma(t)$ shown in Fig. 2, i.e., they have an initial rapid decay followed by a long time tail on the 10–20% level. Also, the different parts of their tails look similar to the corresponding results for $\Gamma(t)$ (see Fig. 2 in II).

Considering then Γ^d_{11} this function will in general show more structure than the two separate parts above. In Fig. 5 we show $\Gamma^d_{11}(qt)/\Gamma^d_{11}(q,t=0)$ (full curves) for four different q values. Except for the lowest-q value where Γ^d_{11} looks similar to $\Gamma(t)$, the tail has more structure and gives also a relatively larger contribution. The dashed curves in Fig. 5 show our previous results for Γ^d_{11} taken from paper IV. We see that there are large differences between our present and earlier results, especially at small times. The reason for this is that our earlier approximation for Γ^d_{11} did not reproduce the exact initial mation for Γ^d_{11} did not reproduce the exact initial value $\Gamma^d_{11}(q,t=0)$, as is the case in the present

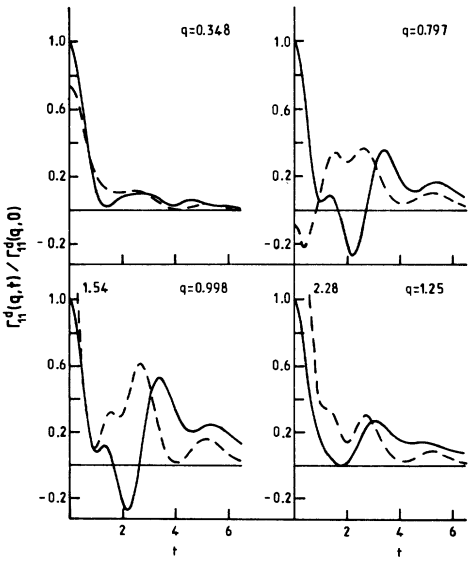

FIG. 5. $\Gamma^d_{11}(qt)/\Gamma^d_{11}(q,t=0)$ versus time. The full curves show the results from the present theory, and the dashed curves are the results from the earlier calculations in paper IV. The latter curves are normalized to the exact value of $\Gamma^d_{11}(q,t=0)$ and the figures in the upper left corner indicate the value at $t=0$.

treatment. These large discrepancies at short times explains why our earlier results for $S(q\omega)$ were rather bad for small and intermediate wave vectors. For $q<1$ we can write $F(qz)$ in a generalized hydrodynamic form [see IV: (2.7) and (2.8)]

$$F(qz)=S(q)\frac{z+q^2\alpha(qz)}{z^2+[q^2/\beta mS(q)]+zq^2\alpha(qz)}, \tag{3.1}$$

where the generalized friction coefficient α is essentially given by

$$\begin{aligned}\alpha(qz)&=[\Gamma(z)+\Gamma^d_{11}(qz)]/q^2\\ &\simeq[\omega_0^2+\Gamma^d_{11}(q,t=0)]/q^2\\ &\times\int_0^\infty dt\exp\left[-\left(zt+\frac{t^2}{\tau_s^2(q)}\right)\right]\end{aligned} \tag{3.2}$$

considering in the last step only the contribution from the binary part. For the smallest-q value in Fig. 5 it is clear that the two curves have essentially the same relaxation time τ_s. We can also take $z=0$ in this case, and we then see that the viscosity depends sensitively on the value of $\Gamma^d_{11}(q,t=0)$. In our earlier results, this value is 25% too small in magnitude at $q=0.35$ and this gives a value for $\alpha(0,0)$, which is a factor of two larger compared with what is obtained with the exact value of $\Gamma^d_{11}(q,t=0)$. This then explains why our earlier results for $S(q\omega)$ were strongly overdamped for smaller-q values. For the intermediate q values around $q\simeq 1$ the frequency dependence of $\alpha(qz)$ is also important, and this depends on the whole time dependence for short and intermediate times. We found earlier that Γ^d_{11} gave a negative contribution to the damping at the frequency of the resonance for $q=1$ [see Fig. 11(d) in IV], while in the present case this contribution is positive at this frequency. This increased damping explains why the peak has been broadened in the present case.

To investigate the time dependence of the different contributions to the tail of Γ^d_{11} we write (2.4) as

$$\begin{aligned}\Gamma^s_{11}(qz)&=\Gamma^{sB}_{11}(qz)+R^s_{00}(qz)+[\Gamma^{sB}_{11}(qz)+\Gamma^s_{11}(qz)]R^s_{01}(qz)\\ &+\Gamma^{sB}_{11}(qz)R^s_{11}(qz)\Gamma^s_{11}(qz)+\Gamma^{sB}_{11}(qz)R^s_{22}(qz)\Gamma^s_{11}(qz)\\ &=\Gamma^{sB}_{11}(qz)+\Gamma^s_{nn}(qz)+\Gamma^s_{nl}(qz)\\ &+\Gamma^s_{ll}(qz)+\Gamma^s_{tt}(qz)\end{aligned} \tag{3.3}$$

and correspondingly for Γ_{11} in (2.14). In Fig. 6 we show the different relative contributions to the tails. The full curves show $\Gamma^d_{nn}=\Gamma_{nn}-\Gamma^s_{nn}$ versus time. The dashed curves show the time dependence of Γ^d_{nl}, the dashed-dot that of Γ^d_{ll}, and the dotted curves that of Γ^d_{tt}. All curves in Fig. 6

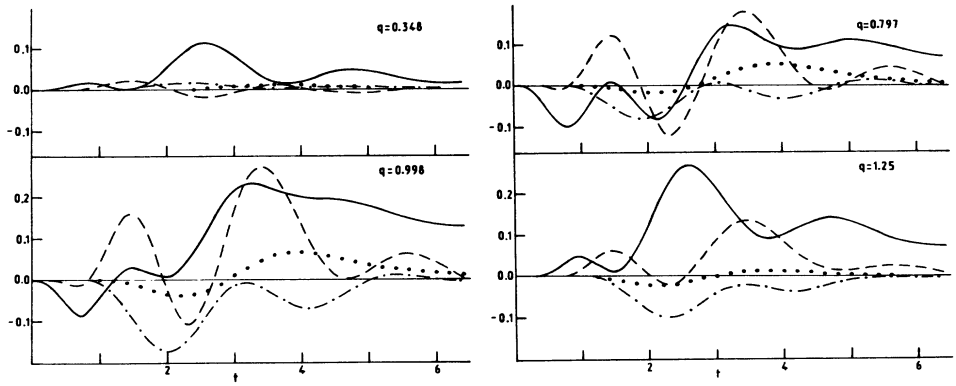

FIG. 6. The different parts of the tail in Γ^d_{11} defined via Eq. (3.3) and a corresponding equation for Γ_{11}. The full curves show $\Gamma^d_{nn}(qt)$, the dashed curves show $\Gamma^d_{nl}(qt)$, the dashed-dot curves show $\Gamma^d_{ll}(qt)$, and the dotted curves show $\Gamma^d_{tt}(qt)$. All curves are normalized with respect to $\Gamma^d_{11}(q, t=0)$.

are normalized with respect to $\Gamma^d_{11}(q, t=0)$. The strong oscillations in the parts representing the density and longitudinal current reflect of course the strong density oscillations in $F(qt)$. The detailed time dependence is for short times sensitive to our explicit choice of F^B in Eq. (2.10), and the negative region around $t=2$ is probably overestimated since this reflects the too high value of $\Gamma(t)$ for the same times. For longer times, F^B has decayed and does not affect the results. The full curves in Fig. 6 should for longer times ($t>3$) be identical with the dashed ones in Fig. 5, since they both represent the coupling to the density fluctuations in the tail. The numerical differences seen originate from different input values for $F(qt)$, where the dashed curves in Fig. 5 were obtained with Lovesey's[17] approximation for $F(qt)$ (cf. Fig. 2 in II).

A large part of the contribution to the tail is for all q values given by Γ^d_{nn}. The two contributions Γ^d_{nl} and Γ^d_{ll} are also relatively large but there is some cancellation between them. The coupling to the currents have obviously a maximum for intermediate q values. This behavior can be understood from physical arguments. Every single atom in the fluid is locally surrounded by a backflow built up of the surrounding atoms, and the single atom plus its local backflow may be referred to as a quasiparticle. The dynamics of the backflow is described by Γ^d_{11} and the single particle motion by Γ. For wave vectors in the interval $q_0/2 < q < q_0$, where q_0 gives the position of the first peak in $S(q)$, the local structure of the quasiparticle is resolved. For these wave vectors one therefore expects a relatively strong coupling to the local flow pattern built up of the currents around the single atom. For smaller wave vectors the average effect due to several quasiparticles is probed, and the local currents around different particles will to a large extent cancel each other. In the other limit of larger-q values the detailed flow pattern cannot be resolved, and the dynamics are governed by fewer and fewer particles, whereby the picture of a collective backflow will be less valid. Eventually only the single particle motion is important and in this limit Γ^d_{11} vanishes.

In Figs. 7(a) and 7(b) we have plotted the area under $\Gamma^d_{11}(qt)$, i.e., $\Gamma^d_{11}(q, z=0)$, together with the different contributions shown in Fig. 6. The dots in Fig. 7(a) show $\Gamma^d_{11}(q, z=0)$ (cf. Fig. 9(b) in IV), the open circles show $\Gamma^{dB}_{11}(q, z=0)$, and the filled squares $\Gamma^d_{nn}(q, z=0)$. The total coupling to the longitudinal currents $\Gamma^d_{nl}(q, z=0)+\Gamma^d_{ll}(q, z=0)$ is shown by open squares. In Fig. 7(b) we show the relative contributions to the area, and the dif-

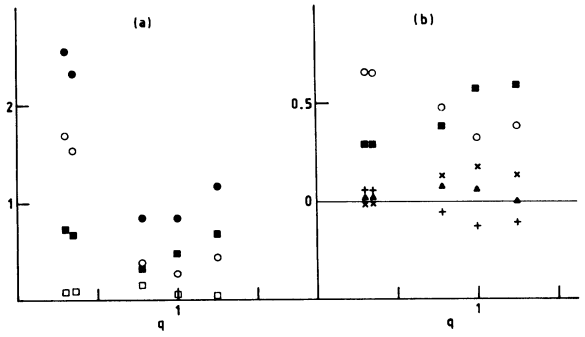

FIG. 7. (a) $-\Gamma^d_{11}(q, z=0)$ (filled circles) versus q. Also shown is $-\Gamma^{dB}_{11}(q, z=0)$ (open circles), $-\Gamma^d_{nn}(q, z=0)$ (filled squares), and $-\Gamma^d_{nl}(q, z=0)-\Gamma^d_{ll}(q, z=0)$ (open squares). The vertical axis is in units of τ_0^{-1}. (b) The normalized contributions to $\Gamma^d_{11}(q, z=0)$. The open circles and filled squares correspond to those in (a). The crosses show $\Gamma^d_{nl}(q, z=0)/\Gamma^d_{11}(q, z=0)$, the pluses show the corresponding contribution from Γ^d_{ll}, and the filled triangles show that from Γ^d_{tt}.

ferent parts Γ^d_{nl} and Γ^d_{ll} are shown separately by crosses and pluses, respectively. The filled triangles show the contribution from Γ^d_{tt}, while the other symbols refer to those in Fig. 7(a). The variation in the area of $\Gamma^d_{11}(qt)$ with q reflects the local static structure of the system, which shows up in the initial value $\Gamma^d_{11}(q, t=0)$. The same typical variation is found for Γ^d_{nn}, which follows from the q dependence of the coupling constants in (2.9) and (2.16). From Fig. 7 we also see that the currents give a maximum contribution around $q=0.8$ but the effect of this on $S(q\omega)$ is relatively small. The large cancellation between the longitudinal currents is clearly seen in Fig. 7(b).

IV. DISCUSSION

The results presented in this paper show that our kinetic theory derived in papers I and III gives almost quantitative agreement with MD and experimental results both for the self-motion shown in Fig. 2 and for the collective density fluctuations shown in Fig. 3. It is clear from Figs. 3 and 4 that at the present density and temperature this agreement can be obtained by just including the binary part and the mode-mode term R_{00} in the memory functions, and the same conclusion holds also for the self-motion. This situation would, however, change when we go to lower densities. Consider, for instance, the diffusion constant. This shows a characteristic density dependence relative to its binary or Enskog value, as has been shown in MD calculations by Alder *et al.*[18] and by Levesque and Verlet.[19] The enhancement over its binary value at low and intermediate densities have been found to come from the coupling to the vortex flow introduced by R_{22}, (Ref. 20) which dominates the tail at lower densities. It would therefore be desirable to test the present theory also for lower density systems, to see whether our approximations for R_{01}, R_{11}, and R_{22} can give quantitative agreement also in that case.

The overall magnitude of the dominant terms R^s_{00} and R^l_{00} in the tail can be estimated to be proportional to $1/S(0)$ if $S(0) \ll 1$ [see III: (4.3)], i.e., inversely proportional to the compressibility. The relatively large time tails in rubidium is, therefore, like the existence of the sharp side peaks in $S(q\omega)$, due to the relatively small compressibility for this system. The corresponding physical picture is the so-called cage effect. Every atom is, at high density, to some extent trapped in a cage of surrounding atoms and this effect will be more pronounced the lower the compressibility is. Lowering the temperature of the system, we therefore expect that the R_{00} terms will develop a larger and more long-lived tail, which eventually gives a nearly constant plateau in the memory functions. This will then correspond to an amorphous solid. In the opposite limit of lower density and higher temperature, the cage effect will be reduced and the particles will be more free to move, whereby the couplings to the currents become more important.

Consider argon, which has a higher compressibility; we expect the tails to be reduced, at least at high densities. This is confirmed by MD calculations and it was also found in our previous calculations in II. This implies that while rubidium cannot be described by a memory function with just a single relaxation time,[6] this may be a better approximation for argon. In this connection we should also notice that the value $S(q, \omega=0)$ to a large extent reflects the time dependence of the tail, and cannot therefore be used to fix a relaxation time for the binary part.

The self-part F^s has here, as before in IV, been treated within the Gaussian approximation. It is known that this gives systematic deviations from the MD results[21] for intermediate q values. It seems, however, possible to formulate a theory also for this function within the present formulation. It would then also be desirable to perform a fully self-consistent calculation of the mode-mode integrals and make a systematic investigation of the dependence of the results on the state considered and also on the interatomic potential. We hope to come back to these questions in future publications.

ACKNOWLEDGMENTS

The author would like to thank Dr. A. Rahman for providing his MD data on rubidium. This work has been supported by the Swedish Natural Science Research Council.

[1] L. Sjögren and A. Sjölander, J. Phys. C 12, 4369 (1979); referred to as I.

[2] L. Sjögren, J. Phys. C 13, 705 (1980); referred to as II.

[3] L. Sjögren, Phys. Rev. A 22, 2866 (1980); referred to as III.

[4] A. Rahman, Phys. Rev. Lett. 32, 52 (1974); Phys. Rev. A 9, 1667 (1974).

[5] J. R. D. Copley and J. M. Rowe, Phys. Rev. Lett. 32, 49 (1974); Phys. Rev. A 9, 1656 (1974).

[6] P. K. Kahol, R. Bansal, and K. N. Pathak, Phys. Rev.

A 14, 408 (1976); P. K. Kahol and D. K. Chaturwedi, *ibid.* 18, 2717 (1978).
[7]M. I. Barker and T. Gaskell, J. Phys. C 8, 3715 (1975).
[8]F. Yoshida, J. Phys. F 8, 411 (1978); F. Yoshida and S. Takeno, J. Phys. C 11, 2895 (1978).
[9]T. Nishigori, J. Stat. Phys. 20, 83 (1979).
[10]J. Bosse, W. Götze, and M. Lücke, Phys. Rev. A 18, 1176 (1978); A. Zippelius and W. Götze, *ibid.* 17, 414 (1978).
[11]S. Sjödin and A. Sjölander, Phys. Rev. A 18, 1723 (1978).
[12]L. Sjögren and A. Sjölander, Ann. Phys. (N.Y.) 110, 421 (1978); referred to as IV.
[13]W. C. Kerr, Phys. Rev. 174, 316 (1968); K. S. Singwi, K. Sköld, and M. P. Tosi, Phys. Rev. A 1, 454 (1970).
[14]L. Sjögren and A. Sjölander, Ann. Phys. (N.Y.) 110, 122 (1978).
[15]D. L. Price, K. S. Singwi, and M. P. Tosi, Phys. Rev. B 2, 2983 (1970).
[16]M. Nelkin and S. Ranganathan, Phys. Rev. 164, 222 (1967).
[17]S. W. Lovesey, Phys. Lett. A36, 413 (1971); see also, J. R. D. Copley and S. W. Lovesey, Rep. Prog. Phys. 38, 461 (1975).
[18]B. J. Alder, D. M. Gass, and T. E. Wainwright, J. Chem. Phys. 53, 3813 (1970).
[19]D. Levesque and L. Verlet, Phys. Rev. A 2, 2514 (1970).
[20]P. Resibois, J. Stat. Phys. 13, 393 (1975); R. I. Cukier and J. R. Mehaffey, Phys. Rev. A 18, 1202 (1978).
[21]W. Götze and A. Zippelius, Phys. Rev. A 14, 1842 (1976).